Science Signaling AAAS

www.sciencesignaling.org/cgi/content/full/4/194/ra67/DC1

Supplementary Materials for

Load-Induced Modulation of Signal Transduction Networks

Peng Jiang, Alejandra C. Ventura, Eduardo D. Sontag, Sofia D. Merajver, Alexander J. Ninfa,* Domitilla Del Vecchio*

*To whom correspondence should be addressed. E-mail: aninfa@umich.edu (A.J.N.); ddv@mit.edu (D.D.V.)

Published 11 October 2011, *Sci. Signal.* **4**, ra67 (2011)
DOI: 10.1126/scisignal.2002152

This PDF file includes:

Text
Fig. S1. Steady-state effects of loading.
Fig. S2. Effect of loading on the frequency response.
Fig. S3. Effects of enzyme amounts.
Fig. S4. Effect of the load on the amplitude of response to a train of pulses.
Fig. S5. Response of the UTase/UR–PII cycle to stimulation with nonsaturating concentrations of glutamine.
Fig. S6. Using glutaminase and injections of glutamine to impose time-varying input stimulation.
Fig. S7. Amplitude of the initial response to glutamine addition depends on whether or not the system has achieved a steady state before glutamine addition.
References

Other Supplementary Material for this manuscript includes the following:
(available at www.sciencesignaling.org/cgi/content/full/4/194/ra67/DC1)

SimulinkModel (.mdl file)

1 Model and Simulation

We consider the covalent modification cycle with its targets as shown in Figure 1 A. Here, we analyze how the targets control the system transient response to the input stimulus u. We consider the standard two-step reaction model for enzymatic reactions [5]. Let E_1 and E_2 be the converter enzymes that convert protein W to its active form W* and protein W* back to the inactive form W, respectively. Let C_1 denote the complex of E_1 with W and C_2 be the complex of E_2 with W*. The reactions describing the system are given by

$$\mathrm{W} + \mathrm{E}_1 \underset{d_1}{\overset{a_1}{\rightleftharpoons}} \mathrm{C}_1 \xrightarrow{k_1} \mathrm{W}^* + \mathrm{E}_1$$

$$\mathrm{W}^* + \mathrm{E}_2 \underset{d_2}{\overset{a_2}{\rightleftharpoons}} \mathrm{C}_2 \xrightarrow{k_2} \mathrm{W} + \mathrm{E}_2.$$

Both the inactive and active protein forms bind to targets L and N, respectively, to form complexes $\bar{\mathrm{C}}$ and C, respectively. In Figure 1 A, λ and α denote "effective" loads resulting from the binding to targets and are given by the amounts of targets normalized by their dissociation constants as explained in what follows. We add the binding reaction of W with its targets L $\mathrm{W} + \mathrm{L} \underset{k_{off}}{\overset{k_{on}}{\rightleftharpoons}} \mathrm{C}$, and the binding of W* with its targets N $\mathrm{W}^* + \mathrm{N} \underset{\bar{k}_{off}}{\overset{\bar{k}_{on}}{\rightleftharpoons}} \bar{C}$.

The rate equations governing the system are given by

$$\begin{aligned}
\frac{dW}{dt} &= -a_1 W E_1 + d_1 C_1 + k_2 C_2 - k_{on} L W + k_{off} C \\
\frac{dC_1}{dt} &= a_1 W E_1 - (d_1 + k_1) C_1 \\
\frac{dW^*}{dt} &= -a_2 W^* E_2 + d_2 C_2 + k_1 C_1 - \bar{k}_{on} N W^* + \bar{k}_{off} \bar{C} \\
\frac{dC_2}{dt} &= a_2 W^* E_2 - (d_2 + k_2) C_2 \\
\frac{dC}{dt} &= k_{on} L W - k_{off} C \\
\frac{d\bar{C}}{dt} &= \bar{k}_{on} N W^* - \bar{k}_{off} \bar{C}.
\end{aligned}$$

To this differential equations, we add the algebraic equations expressing the conservation laws for the protein and the enzymes:

$$W_T = W + W^* + C_1 + C_2 + C + \bar{C},\ E_{1T} = E_1 + C_1,\ E_{2T} = E_2 + C_2.$$

Assuming $k_{off}, k_{on}, \bar{k}_{on}, \bar{k}_{off}, a_1, a_2, d_1, d_2 \gg k_1, k_2$ and $W_T \gg E_{1T}, E_{2T}$, we can employ the quasi steady state approximation (QSSA). Hence, we have that $\frac{dC_1}{dt} = 0$, $\frac{dC_2}{dt} = 0$, $\frac{dC}{dt} = 0$, and $\frac{d\bar{C}}{dt} = 0$. From these, we obtain that

$$C_1 = \frac{E_{1T} W}{K_1 + W} \text{ with } K_1 = (d_1 + k_1)/a_1, \quad C_2 = \frac{E_{2T} W^*}{K_2 + W^*} \text{ with } K_2 = (d_2 + k_2)/a_2$$

and that

$$C = L/k_D,\ \bar{C} = N/\bar{k}_D,\ \text{with } k_D = k_{off}/k_{on},\ \bar{k}_D = \bar{k}_{off}/\bar{k}_{on}.$$

Since $\bar{W} = W^* + \bar{C} =$, we have that $\frac{d\bar{W}}{dt} = \frac{dW^*}{dt} + \frac{d\bar{C}}{dt} = -a_2 W^* E_2 + d_2 C_2 + k_1 C_1$, so that

$$\frac{d\bar{W}}{dt} = -a_2 W^* \frac{K_2 E_{2T}}{K_2 + W^*} + d_2 W^* \frac{E_{2T}}{K_2 + W^*} + k_1 \frac{E_{1T} W}{K_1 + W}.$$

Letting $\lambda := \frac{L}{k_D}$, $\alpha := \frac{N}{k_D}$, considering that $a_2 K_2 = d_2 + k_2$, $W^* = \bar{W}/(1+\alpha)$, and $W = (W_T - \bar{W})/(1+\lambda)$, we finally obtain

$$\frac{d\bar{W}}{dt} = V_1 \frac{W_T - \bar{W}}{K_1(\lambda+1) + (W_T - \bar{W})} - V_2 \frac{\bar{W}}{K_2(1+\alpha) + \bar{W}}, \tag{1}$$

in which $V_1 = k_1 E_{1T}$ and $V_2 = k_2 E_{2T}$ are the speeds of modification. Note that in the case in which $\alpha = 0$, we have that $\bar{C} = 0$ and we obtain as a special case of our derivations the situation in which the load is applied only to W.

This is the same differential equation as obtained in [2], in which the Michaelis-Menten constants are multiplied by a factor that increases with the amounts of downstream load. When $\lambda = \alpha = 0$, we obtain the differential equation for the system without the downstream load. Note that the differential equation for the free active protein concentration W^* would differ. Here, we focus on the total active protein dynamics because it is what can be measured in our experimental system.

Furthermore, if we assume that the activity of the enzymes are regulated by an allosteric effector u, which acts, for example, as an absolute activator for E_2 and as a non-competitive inhibitor for E_1, we obtain the following ordinary differential equation (ODE) model:

$$\frac{d\bar{W}}{dt} = \frac{V_1}{(1 + u/k'_D)} \frac{W_T - \bar{W}}{K_1(1+\lambda) + (W_T - \bar{W})} - V_2 \left(\frac{u}{\bar{k}'_D + u} \right) \frac{\bar{W}}{K_2(1+\alpha) + \bar{W}}, \tag{2}$$

in which k'_D and $\bar{k}'_D$ are the dissociation constants for the binding of u with E_1 and E_2, respectively. This model is also the same as the one of [2], in which the Michaelis-Menten constants are multiplied by factors that depend on the load. In this model, the (time-varying) input stimulus is given by $u(t)$. The results that we will obtain regarding the effects of the load on the dynamic response of $\bar{W}(t)$ to $u(t)$ are independent on whether there is an allosteric effector that regulates the activity of the enzymes. Specifically, similar results can be obtained for model (1) in which the input stimulus is given by $V_2(t)$ or by $V_1(t)$. Since in the experimental system, the input stimulus is an allosteric effector, we will carry the detailed analysis for this case.

1.1 Effects of the load on the steady state input/output response: stoichiometric retroactivity

In order to understand the effect of the load on the dynamic response of the system, we first recall the effect of sequestering by downstream targets on the steady states of an upstream system, that is, stoichiometric retroactivity [7] . Solving the ODE model (2) for the equilibrium by setting $\frac{d\bar{W}}{dt} = 0$, we obtain that $\bar{W}$ satisfies the equation

$$S = \frac{(W_T - \bar{W})(K_2(1+\alpha) + \bar{W})}{\bar{W}(K_1(1+\lambda) + W_T - \bar{W})}, \tag{3}$$

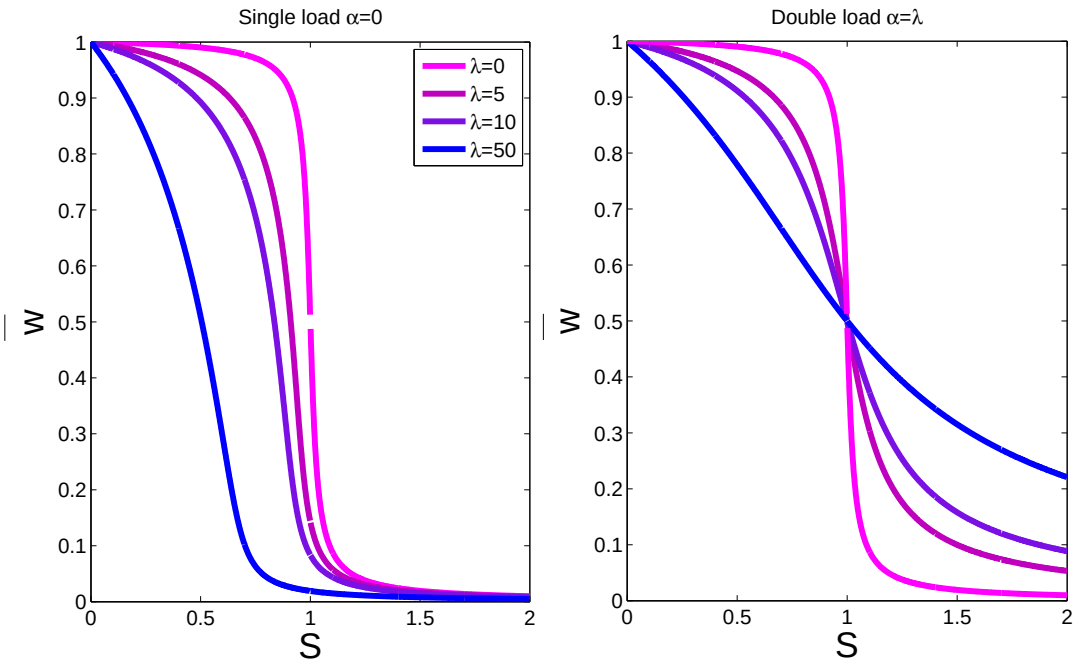

Figure S 1: **Steady state effects of loading.** Left: Effect of L_T on the steady state response of $\bar{W}$ to u when the load is applied only to W, that is, $N = 0$ so that $\alpha = 0$. Right: Effect of the load N on the steady state response of $\bar{W}$ to u when the load is applied to both W and W^*, and L=N, $k_D = \bar{k}_D = 1$, $K_1 = K_2 = 0.01$ and $W_T = 1$.

in which $S = V_2 \left(\frac{u}{k'_D+u}\right) / \left(\frac{V_1}{(1+u/k'_D)}\right)$. We plot in Figure S 1 the steady state values of $\bar{W}$ for varying amounts of S (the reader is referred to [7] for more details). In the case in which the load is applied on both W and W^*, the curves with different values of load cross all at the same point. This can be shown as follows. Assuming that L=N, that is, the downstream target is the same for both W and W*, which is the case in the experimental system, we have that $\alpha = \lambda \frac{\bar{k}'_D}{\bar{k}_D}$. Hence, we can re-write equation (3) as

$$S(\lambda, \bar{W}) = \frac{(W_T - \bar{W})(K_2(1 + \lambda \frac{\bar{k}'_D}{\bar{k}_D}) + \bar{W})}{\bar{W}(K_1(1+\lambda) + W_T - \bar{W})}.$$

For the family of curves in the (S, λ) plane to cross all at the same point for different values of λ, we have to request that there is a value $\bar{W}_0$, not dependent on α, such that $\frac{\partial S}{\partial \lambda}(\lambda, \bar{W}_0) = 0$. This gives:

$$\bar{W}_0 = \frac{K_2(\frac{\bar{k}'_D}{\bar{k}_D} K_1 + \frac{\bar{k}'_D}{\bar{k}_D} W_T - K_1)}{K_2 \frac{\bar{k}'_D}{\bar{k}_D} + K_1},$$

which is acceptable if and only if

$$\frac{\bar{k}'_D}{\bar{k}_D} K_1 + \frac{\bar{k}'_D}{\bar{k}_D} W_T - K_1 > 0 \text{ and } K_2 K_1 \frac{\bar{k}'_D}{\bar{k}_D} - K_2 K_2 - W_T K_1 < 0.$$

If this condition on the parameters is satisfied, then all steady state characteristics cross at the same point for varying amounts of load.

The qualitative effect of increasing the load, when applied to both sides, is to make the steady state response of the system linear for larger input variations about the crossing point. When the load is applied to one side only, that is, $\alpha = 0$, the major effect of the load is on the decrease of the value of the S_{50}, that is, the value of S corresponding to half-maximal response.

1.2 Characteristics of the dynamic response

In order to characterize the effect of the load on the dynamic response of the system, that is, load-induced modulation, we quantify the rise time, the decay time, the bandwidth and amplitude of response as functions of the load. Specifically, we define these quantities as follows. Let W_0 be the initial state of the cycle, that is, $W(0) = W_0$ and let W_{eq} be the steady state value corresponding to a constant input stimulus u.

Decay time. If $W_0 > W_{eq}$, we define the decay time as

$$t_{decay} = t_{10} - t_{90},$$

in which

$$t_{10} = \{t \mid \bar{W}(t) = W_0 + 0.9(W_{eq} - W_0)\}, \text{ and } t_{90} = \{t \mid \bar{W}(t) = W_0 + 0.1(W_{eq} - W_0)\}.$$

Rise time. if $W_0 < W_{eq}$, we define the rise time as

$$t_{rise} = t_{90} - t_{10},$$

in which

$$t_{90} = \{t \mid \bar{W}(t) = W_0 + 0.9(W_{eq} - W_0)\}, \text{ and } t_{10} = \{t \mid \bar{W}(t) = W_0 + 0.1(W_{eq} - W_0)\}.$$

Basically, the rise time quantifies the time $\bar{W}$ takes to rise from 10% of its overall excursion $|W_{eq} - W_0|$ to 90% of it, while the decay time quantifies the time $\bar{W}$ takes to decay from 90% of its overall excursion $|W_{eq} - W_0|$ to 10% of it. Other definitions of rise and decay times consider excursions of the signal between 5% and 95% or between 1% and 99%. The results of this paper do not depend on these specific values.

Bandwidth. Consider a periodic input stimulus $u(t)$ with period T. Let $\omega := \frac{2\pi}{T}$ be the frequency of the input stimulus and $A(\omega)$ be the amplitude of the permanent response of $\bar{W}(t)$ corresponding to input frequency ω. Note that it can be formally shown that the permanent response exists for the reduced system in equation (2) (see [6], for example). Let $A(0)$ be the amplitude of response when $\omega \to 0$. Then, the bandwidth of the system, denoted ω_B, is defined as the frequency at which the amplitude drops below $1/\sqrt{2}A(0)$, that is, ω_B is such that

$$A(\omega_B) = \frac{A(0)}{\sqrt{2}}.$$

The bandwidth of a system indicates how frequently a time-varying input stimulus can change before the system becomes incapable of responding to it. The bandwidth is usually calculated by applying small amplitude sinusoidal input stimuli at different frequencies and by measuring the

corresponding amplitude of response. Even though sinusoidal input stimuli are not necessarily biologically relevant, the system response to these inputs provides information on the amplitude of response and bandwidth even for more complicated input profiles. We therefore base our analysis on these types of inputs. However, since input profiles that have the shape of train of pulses are most often found in practice and in particular in our experiments, we complement our analysis on sinusoidal input stimuli with an analysis that considers the effect of both the period and the shape of the pulse profile on the system response.

1.3 Load-induced modulation of rise and decay times

We first consider the times the cycle takes to switch between "off" (fully unmodified) and "on" (fully modified) states in response to extreme inputs u, that is, $u = 0$ or $u \approx \infty$. When the inputs are extreme, the modification rates in equation (2) do not depend on the input u anymore as the modification speeds saturate to their extreme values. In this case, we say that the cycle operates in the zero-order regime. We then turn our attention to consider the transition time between states corresponding to intermediate values of the input u for which the modification speeds are not saturated. In this case, we say that the cycle operates in the first-order regime.

1.3.1 Transition times between "on" and "off" states

For the decay time, we have that the final steady state is $W_{eq} = 0$ corresponding to $u = \infty$ and the initial steady state value is $W_0 = W_T$ corresponding to $u = 0$. For the rise time, we have that the final steady state is $W_{eq} = W_T$ corresponding to $u = 0$ and the initial steady state is $W_0 = 0$ corresponding to $u = \infty$.

Decay time. For sufficiently large input stimuli u, we have that $\frac{V_1}{(1+u/k'_D)} \approx 0$ and that $\frac{u}{k'_D+u} \approx 1$, so that equation (2) reduces to

$$\frac{d\bar{W}}{dt} = -V_2 \frac{\bar{W}}{K_2(1+\alpha) + \bar{W}}, \ \bar{W}(0) = W_T. \tag{4}$$

This differential equation can be directly integrated through the method of separation of variables as follows. Re-write it as

$$\frac{K_2(1+\alpha) + \bar{W}}{\bar{W}} d\bar{W} = -V_2 dt,$$

which, integrating the left-hand side between $\bar{W} = \bar{W}(0)$ and $\bar{W} = \bar{W}(t)$ and the right-hand side between $t = 0$ and t yields

$$\int_{\bar{W}(0)}^{\bar{W}(t)} \left(\frac{K_2(1+\alpha)}{\bar{W}} + 1 \right) d\bar{W} = -V_2 t,$$

which yields to

$$K_2(1+\alpha)(\ln(\bar{W}(t)) - \ln(\bar{W}(0))) + \bar{W}(t) - \bar{W}(0) = -V_2 t.$$

This, in turn yields to

$$t = \frac{1}{V_2} \left(K_2(1+\alpha) \ln\left(\frac{W_T}{\bar{W}(t)} \right) + W_T - \bar{W}(t) \right). \tag{5}$$

From this expression, we can approximate t_{10} and t_{90} by

$$t_{10} = \frac{1}{V_2}\left(K_2(1+\alpha)\ln(10) + 0.9W_T\right) \text{ and } t_{90} = \frac{1}{V_2}\left(K_2(1+\alpha)\ln(1.1) + 0.1W_T\right),$$

so that

$$t_{decay} = \frac{1}{V_2}\left(K_2(1+\alpha)\ln(10/1.1) + 0.8W_T\right). \tag{6}$$

Therefore, since $\alpha > 0$, the system with load applied to W^* displays an increased decay time compared to the system with no load applied to W^*. Furthermore, the decay time increases with the total amount of protein W_T and with the Michaelis-Menten constant K_2 of the reverse covalent modification reaction, while increasing the amount of enzyme E_2 decreases the decay time. Also, note that the decay time only depends on the parameters of the reverse covalent modification reaction.

Rise time. For sufficiently small input stimuli, we have that $\frac{V_1}{(1+u/k'_D)} \approx V_1$ and that $\frac{u}{k'_D+u} \approx 0$, so that equation (2) reduces to

$$\frac{d\bar{W}}{dt} = V_1\frac{W_T - \bar{W}}{K_1(1+\lambda) + (W_T - \bar{W})},\ \bar{W}(0) = 0. \tag{7}$$

This differential equation can be directly integrated using the method of separation of variables as follows. Let $w := W_T - \bar{W}$, then the above ODE in the new variable w becomes

$$\frac{dw}{dt} = -V_1\frac{w}{K_1(1+\lambda) + w},\ w(0) = W_T,$$

which yields to

$$K_1(1+\lambda)\frac{w(t)}{w(0)} + w(t) - w(0) = -V_2 t,$$

in which, substituting $w(t) = W_T - \bar{W}(t)$ and $w(0) = W_T$ finally gives

$$K_1(1+\lambda)\frac{W_T}{W_T - \bar{W}(t)} + \bar{W}(t) = V_2 t.$$

This, in turn yields to

$$t = \frac{1}{V_1}\left(K_1(1+\lambda)\ln\left(\frac{W_T}{W_T - \bar{W}(t)}\right) + \bar{W}(t)\right) \tag{8}$$

From this expression, we can approximate t_{10} and t_{90} by

$$t_{10} = \frac{1}{V_1}\left(K_1(1+\lambda)\ln(1.1) + 0.1W_T\right) \text{ and } t_{90} = \frac{1}{V_1}\left(K_1(1+\lambda)\ln(10) + 0.9W_T\right),$$

so that

$$t_{rise} = \frac{1}{V_1}\left(K_1(1+\lambda)\ln(10/1.1) + 0.8W_T\right). \tag{9}$$

Therefore, since $\lambda > 0$, the system with load applied to W displays an increased rise time compared to the system with no load applied to W. Furthermore, the rise time increases with

the total amount of protein W_T and with the Michaelis-Menten constant K_1 of the forward covalent modification reaction, while increasing the amount of enzyme E_1 decreases the rise time. Also, note that the rise time only depends on the parameters of the forward covalent modification reaction. The results are summarized in Figure 2 A.

Remark. A similar result on the rise and decay times can be obtained for more general dynamic equations using the comparison theorem for scalar ordinary differential equation [1]. Specifically, consider the scalar equation

$$\dot{x} = f_\lambda(x, u) - g_\alpha(x, u),$$

in which we assume that $f \equiv 0$ when $u = \infty$ and that $g \equiv 0$ when $u = 0$. Furthermore, we assume that if $\lambda_1 < \lambda_2$ and $\alpha_1 < \alpha_2$ then $f_{\lambda_1}(x, u) > f_{\lambda_2}(x, u)$ and $g_{\alpha_1}(x, u) > g_{\alpha_2}(x, u)$. Without loss of generality, we assume that $\dot{x} = f_\lambda(x, u)$ has $x = 1$ as global attractor and that $\dot{x} = -g_\alpha(x, u)$ has $x = 0$ as global attractor. Hence, if we start from initial condition $x(0) < 0.1$ and $u = 0$, we have that the solution of $\dot{x} = f_0(x, u)$ will always be larger for any t than the solution of $\dot{x} = f_\lambda(x, u)$ for all $\lambda > 0$. As a consequence, the rise time will be smaller when $\lambda = 0$, that is, for the unloaded system. Similarly, if we start from initial condition $x(0) = 0.9$ and $u = \infty$, we have that the solution of $\dot{x} = -g_0(x, u)$ will always be smaller for any t than the solution of $\dot{x} = -g_\alpha(x, u)$ for all $\alpha > 0$. As a consequence, the decay time will be smaller when $\alpha = 0$, that is, for the unloaded system.

Remark. Note that if one had taken the definition of rise and decay times based on different percentages from 10% and 90%, say x% and y%, one would have obtained for the decay and rise times:

$$t_{decay} = \frac{1}{V_2}\left(K_2(1+\alpha)\ln(x/y) + (0.0y - 0.0x)W_T\right)$$

and

$$t_{rise} = \frac{1}{V_1}\left(K_1(1+\lambda)\ln((1-0.0x)/(1-0.0y)) + (0.0y - 0.0x)W_T\right),$$

which have the same behavior as expressions (6),(9).

1.3.2 Transition times between intermediate states

We next investigate the relationship between the rise and decay times for the isolated and connected systems when the input stimulus u is set to some intermediate value. For this sake, define

$$v_1 := \frac{V_1}{(1 + u/k'_D)} \text{ and } v_2 := V_2\left(\frac{u}{\bar{k}'_D + u}\right),$$

which represent the maximal speeds of the forward and reverse modification reactions, respectively, for a given value of the allosteric effector concentration u. Here, we seek to show that when the isolated system is ultrasensitive, that is, $K_1, K_2 \ll W_T$, if W_0 and W_{eq} are not too small nor too close to W_T, we have that the connected system rise and decay times become smaller than those of the isolated system when $v_1 - v_2 \to 0$ for sufficiently high load. Specifically, as the value of u is changed to make the maximal modification speeds approach each other, then (for sufficiently large loads) we have that the isolated system transient response becomes slower than the connected system transient response. We make this precise by mathematically stating our assumptions as follows.

Assumptions. The isolated system is ultrasensitive, that is, $K_1, K_2 \ll W_T$, and the initial condition W_0 and equilibrium value W_{eq} of $\bar{W}$ satisfy $(W_T - W_0), (W_T - W_{eq}) \gg K_1$ and $W_0, W_{eq} \gg K_2$. Furthermore, we assume that the load is large enough so that $\bar{K}_1 \gg W_T$ and $\bar{K}_2 \gg W_T$.

Claim 1. *Under the above stated assumptions, for $(v_1 - v_2)$ sufficiently small we have that $t^C_{rise} < t^I_{rise}$ and $t^C_{decay} < t^I_{decay}$, in which "I" stands for "Isolated" and "C" Stands for "Connected".*

Proof. Isolated system. Under the above stated assumptions, we have that $K_1 \ll (W_T - \bar{W}(t))$ and $K_2 \ll \bar{W}(t)$ so that, we can approximate system (2) by

$$\frac{d\bar{W}}{dt} \approx v_1 - v_2 \text{ for } 0 < \bar{W}(t) < W_T,$$

and $\frac{d\bar{W}}{dt} = 0$ otherwise, in which $v_1 > v_2$ for u sufficiently small and $v_1 < v_2$ for u sufficiently large. This equation can be integrated to obtain that $\bar{W}(t) = W_0 + (v_1 - v_2)t$, which holds while $\bar{W}(t) < W_{eq}$ for $(v_1 - v_2) > 0$ and while $\bar{W}(t) > W_{eq}$ for $(v_1 - v_2) < 0$. The rise and decay times can be computed employing the definition, which leads to

$$t^I_{rise} = 0.8\frac{W_{eq} - W_0}{v_1 - v_2} \text{ and } t^I_{decay} = 0.8\frac{W_0 - W_{eq}}{v_2 - v_1}.$$

If one had used different percentages in the definition of rise and decay times, the above expression would stay the same except for having a different coefficient in place of 0.8. Note that when $(v_1 - v_2) \to 0$, we have that $W_{eq} \to \frac{W_T K_2}{K_1 + K_2}$, which is a value that does not depend on $(v_1 - v_2)$. Hence, as $(v_1 - v_2) \to 0$, we have that $t_{rise}, t_{decay} \to \infty$, that is, the response becomes arbitrarily slow as v_1 and v_2 approach each other.

Connected system. Here, we consider two cases: $\alpha > 0$ (double load) and $\alpha = 0$ (single load). When $\alpha > 0$, we have that $\bar{K}_1, \bar{K}_2 \gg W_T$ by the assumption, so that we can approximate system (2) by

$$\frac{d\bar{W}}{dt} = \frac{W_T v_1}{\bar{K}_1} - \bar{W}\left(\frac{v_1}{\bar{K}_1} + \frac{v_2}{\bar{K}_2}\right).$$

If instead $\alpha = 0$, we can approximate it by

$$\frac{d\bar{W}}{dt} = \frac{v_1 W_T}{\bar{K}_1} - v_2 - \bar{W}\left(\frac{v_1}{\bar{K}_1}\right).$$

Letting $\delta := \frac{v_1}{\bar{K}_1} + \frac{v_2}{\bar{K}_2}$ when $\alpha > 0$ and $\delta := \frac{v_1}{\bar{K}_1}$ when $\alpha = 0$, the rise and decay times are both equal to

$$t^C_{rise} = t^C_{decay} = \frac{\ln(9)}{\delta}.$$

As a consequence, for a fixed load, there is a sufficiently small value of $v_1 - v_2$ such that $t^C_{rise}, t^C_{decay} < t^I_{rise}, t^I_{decay}$. If one had used different percentages in the definition of rise and decay times, the above expression would stay the same except for having a different coefficient in place of $\ln(9)$.

□

Hence, we can conclude that when the input stimulus u is such that v_1 and v_2 are very close to each other and the isolated system has an ultrasensitive response, then when the load is high enough to move the system to the hyperbolic regime, the connected system response to constant input stimuli is faster than that of the isolated system. Figure 2 B shows how the isolated system response is slower when v_1 and v_2 are closer to each other and how the connected system becomes faster than the isolated system in such a case.

Remark. Note that if $K_1, K_2 \gg W_T$, which implies that the steady state response is hyperbolic, then the loaded system will always be slower even for intermediate values of the input stimulus.

As a final remark on rise and decay times, note that different values of the Michaelis-Menten constants K_1 and K_2 can lead to qualitatively different effects of the load on the rise and decay times for intermediate values of the input stimulation. This point is shown in Figure 2 C. This fact can be explained as follows. Assume first that $V_1 = V_2$. When $v_1/v_2 \gg 1$ or $v_2/v_1 \gg 1$, having $K_1 < K_2$ ($K_2 < K_1$) implies that $t^I_{rise} < t^I_{decay}$ ($t^I_{rise} > t^I_{decay}$) from equations (6,9). Also, with the load, we have that $t^I_{rise} < t^C_{rise}$ and $t^I_{decay} < t^C_{decay}$ from the same equations. With a load α, λ such that $K_1(1+\lambda) \approx K_2(1+\alpha)$ we also have that $t^C_{rise} \approx t^C_{decay}$. When (v_1/v_2) becomes closer to 1, we have (by Claim 1) that t^I_{rise} and t^I_{decay} both increase. Hence, there is a value of (v_1/v_2) for which $t^I_{decay} > t^C_{decay}$ ($t^I_{decay} < t^C_{decay}$) but $t^I_{rise} < t^C_{rise}$ ($t^I_{rise} > t^C_{rise}$). In theory, by making (v_1/v_2) approach 1, also t^I_{rise} (t^I_{decay}) should become larger than t^C_{rise} (t^C_{decay}). In practice, however, there may be limitations to how close to each other v_1 and v_2 can be made. More generally, assume that when $v_1/v_2 \gg 1$ or $v_2/v_1 \gg 1$ we have that $t^I_{rise} < t^I_{decay}$ ($t^I_{rise} > t^I_{decay}$) and that the load is such that $t^C_{rise} \geq t^C_{decay}$. Then, as (v_1/v_2) approaches 1, we have that $t^I_{decay} > t^C_{decay}$ ($t^I_{decay} < t^C_{decay}$) but $t^I_{rise} < t^C_{rise}$ ($t^I_{rise} > t^C_{rise}$) unless (v_1/v_2) is made very close to 1, which is possible in theory but may be practically hard to realize.

1.4 Load-induced modulation of the frequency response

In this section, we study the effect of the load on the response to periodic input stimuli. Specifically, we consider the response to sinusoidal input stimuli both for the isolated and connected systems. In the next section, we consider more general input stimuli to validate the results obtained with sinusoidal inputs.

We consider periodic inputs of the form $u(t) = u_0 + A_0 \sin(\omega t)$, in which $u_0 > A_0$ is the mean value, or bias, A_0 is the amplitude of the signal about the mean, which is supposed to be small, and ω is the frequency, that is, $\omega = 2\pi/T$ in which T is the period of the signal. We compute the amplitude of the response, the bandwidth, and the effect on the amplitude of changes in the amounts of enzymes E_{1T} and E_{2T}. In what follows, we first consider the case in which the system is loaded on both sides, that is, $\alpha \neq 0$ and $\lambda \neq 0$. In this case, we can choose a value of u_0 such that the corresponding steady state values for the isolated and connected systems are the same for all values of load (see right-side plots of Figure S 1). This substantially simplifies the analysis. Let thus the bias term u_0 be such that $(u_0, \bar{W}_0)$ is a steady state for both the isolated and connected systems.

Assuming the amplitude A_0 to be sufficiently small, we can employ the linear approximation of system (2) about the equilibrium $(u_0, \bar{W}_0)$ [3,4]. Letting $\bar{K}_1 := K_1(1+\lambda)$ and $\bar{K}_2 := K_2(1+\alpha)$

to simplify notation, consider the ODE model for the system

$$\frac{d\bar{W}}{dt} = \frac{V_1}{(1+u/k'_D)}\frac{W_T-\bar{W}}{\bar{K}_1+(W_T-\bar{W})} - V_2\left(\frac{u}{\bar{k}'_D+u}\right)\frac{\bar{W}}{\bar{K}_2+\bar{W}},$$

and assume that A_0 is sufficiently small so that the change of $\bar{W}$ about $\bar{W}_0$, that is, $\Delta\bar{W} = \bar{W}-\bar{W}_0$ is small enough so that the dynamics of $\Delta\bar{W}$ are well approximated by the linearization of the above system about $(u_0, \bar{W}_0)$, that is,

$$\frac{d\Delta\bar{W}}{dt} = -\left(\frac{u_0V_2}{\bar{k}'_D+u_0}\frac{\bar{K}_2}{(\bar{K}_2+\bar{W}_0)^2} + \frac{k'_DV_1}{k'_D+u_0}\frac{\bar{K}_1}{(\bar{K}_1+(W_T-\bar{W}_0))^2}\right)\Delta\bar{W} -$$

$$\left(\frac{\bar{k}'_D}{(\bar{k}'_D+u_0)^2}\frac{\bar{W}_0V_2}{\bar{K}_2+\bar{W}_0} + \frac{k'_DV_1}{(k'_D+u_0)^2}\frac{W_T-\bar{W}_0}{\bar{K}_1+(W_T-\bar{W}_0)}\right)A_0\sin(\omega t).$$

Letting

$$\delta = \frac{u_0V_2}{\bar{k}'_D+u_0}\frac{\bar{K}_2}{(\bar{K}_2+\bar{W}_0)^2} + \frac{k'_DV_1}{k'_D+u_0}\frac{\bar{K}_1}{(\bar{K}_1+(W_T-\bar{W}_0))^2} \tag{10}$$

and

$$\beta = \frac{\bar{k}'_D}{(\bar{k}'_D+u_0)^2}\frac{\bar{W}_0V_2}{\bar{K}_2+\bar{W}_0} + \frac{k'_DV_1}{(k'_D+u_0)^2}\frac{W_T-\bar{W}_0}{\bar{K}_1+(W_T-\bar{W}_0)}. \tag{11}$$

this differential equation can be integrated to obtain

$$\Delta\bar{W}(t) = -\frac{A_0\beta}{\sqrt{\omega^2+\delta^2}}\sin(\omega t - \tan^{-1}(\omega/\delta)) - \frac{A_0\beta\omega}{\omega^2+\delta^2}e^{-\omega_B t},$$

from which we obtain the expression of the amplitude

$$A(\omega) = \frac{A_0\beta}{\sqrt{\omega^2+\delta^2}}. \tag{12}$$

We call δ the *cycle flux* and it quantifies the speed of the conversion reactions when the cycle operates in a small neighborhood of the equilibrium point $(u_0, \bar{W}_0)$. Note that it depends on the amount of load. Here, we explicitly consider two different cases based on whether the isolated system has an ultrasensitive response ($K_1, K_2 \ll W_T$) or whether it has a hyperbolic response (K_1, K_2 are comparable to W_T). In fact, the dependency of the cycle flux on the load is qualitatively different in these two cases and will result in different bandwidths.

Case 1 (Double load and ultrasensitive isolated system steady state response: $K_1, K_2 \ll W_T$). In this case, assuming also that $\bar{W}_0, W_T-\bar{W}_0 \gg K_1, K_2$, the expressions of β and δ are well approximated by β^I and δ^I, in which "I" stands for "Isolated", given by

$$\beta^I = \frac{V_1k'_D}{(k'_D+u_0)^2} + \frac{V_2\bar{k}'_D}{(\bar{k}'_D+u_0)^2}, \text{ and } \delta^I = 0.$$

As a consequence, the amplitude for the isolated system response $A^I(\omega)$ is well approximated by

$$A^I(\omega) = \begin{cases} \min\{\bar{W}_0, W_T-\bar{W}_0\} & \text{if } \omega \le \omega_B^I/\sqrt{2} \\ \frac{\beta^I A_0}{\omega} & \text{if } \omega > \omega_B^I/\sqrt{2}, \end{cases} \tag{13}$$

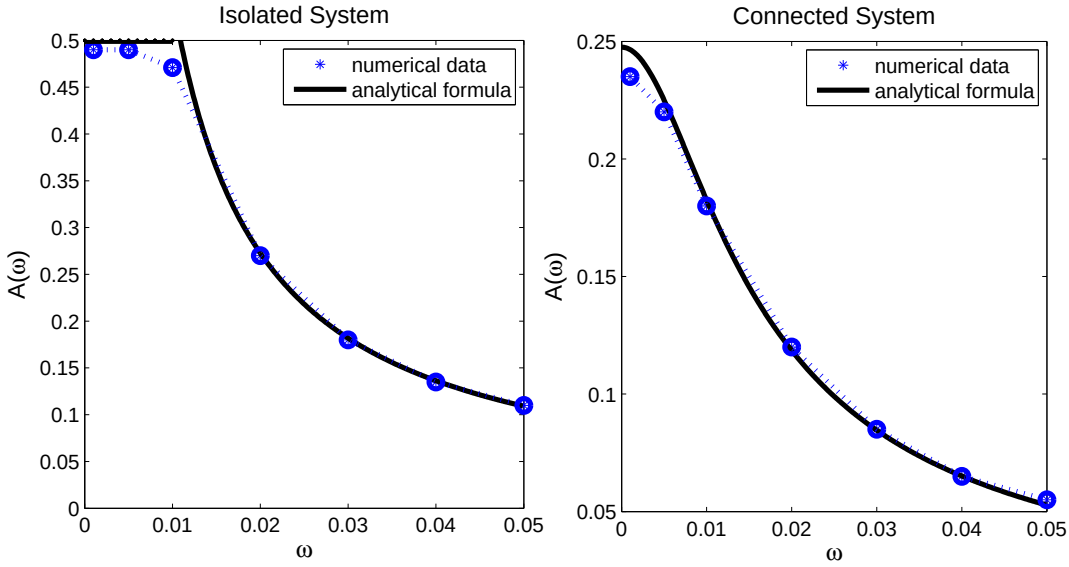

Figure S 2: **Effect of loading on the frequency response.** Numerical simulation data (dashed line) against the analytically predicted values of the amplitudes (solid line) for both the isolated (left) and connected (right) systems from the formulas in equations (13) and (14), respectively. Here, we have set $A_0 = 0.5, u_0 = 1$, $k'_D = \bar{k}'_D = 2$, $K_1 = K_2 = 0.01$, $V_2 = \bar{k}'_D V_1$, $V_1 = 0.01$, $\alpha = \lambda = 50$, $W_T = 1$.

in which

$$\omega_B^I = \frac{\sqrt{2}\beta^I A_0}{\min\{\bar{W}_0, W_T - \bar{W}_0\}}$$

is the bandwidth of the isolated system. For the connected system, if $\frac{A_0\beta^C}{\delta^C} \leq \min\{\bar{W}_0, W_T - \bar{W}_0\}$ then we have that

$$A^C(\omega) = \frac{A_0\beta^C}{\sqrt{\omega^2 + (\delta^C)^2}}, \text{ and } \omega_B^C = \delta^C \tag{14}$$

in which "C" denotes "Connected", and δ^C and β^C are given by the expressions of δ and β given in equations (10)-(11) evaluated at the non-zero load values α and λ. From theory, these expressions hold for A_0 small enough. Figure S 2 shows that in practice these expressions hold for quite large values of A_0. So, in this case, we have that the bandwidth of the connected system is smaller than that of the isolated system, that is, $\omega_B^C < \omega_B^I$ if $\delta^C < \frac{\sqrt{2}\beta^I A_0}{\min\{\bar{W}_0, W_T - \bar{W}_0\}}$, which is satisfied for large enough loads since $\delta^C \to 0$ as $(\lambda, \alpha) \to \infty$. If we have that $\frac{A_0\beta^C}{\delta^C} > \min\{\bar{W}_0, W_T - \bar{W}_0\}$, then the amplitude expression of equation (14) holds only for ω sufficiently large and the bandwidth is not equal to the cycle flux δ^C but to $\omega_B^C = \sqrt{\frac{2A_0^2(\beta^C)^2}{\min\{\bar{W}_0, W_T - \bar{W}_0\}^2} - (\delta^C)^2}$, which is always smaller than ω_B^I. Hence, we conclude that for large enough loads, the bandwidth of the connected system is smaller than that of the isolated system, that is, $\omega_B^C < \omega_B^I$.

Case 2 (Double load and hyperbolic isolated system steady state response: K_1, K_2 comparable with W_T). If $W_T - K_1 \leq \bar{W}_0 \leq K_2$, then the cycle flux δ is a monotonically decreasing function

of the load, therefore we have that $\delta^I > \delta^C$. If A_0 is small enough so that $\frac{A_0\beta^I}{\delta^I}, \frac{A_0\beta^C}{\delta^C} < \min\{\bar{W}_0, W_T - \bar{W}_0\}$, we have that $\omega_B^C = \delta^C$ and $\omega_B^I = \delta^I$ so that for all values of the load $\omega_B^C < \omega_B^I$, that is, the bandwidth of the connected system is always smaller than that of the isolated system.

Case 3 (Single load). We conclude by considering the effect of the load when it is applied only to W, that is, $\alpha = 0$ but $\lambda \neq 0$. In this situation, the equilibrium of the connected system is always lower than the equilibrium of the isolated system for all input values (Figure S 1) and the linear approximation of system (2) holds only for very small values of A_0. Hence, the conclusions of the analysis depend on the specific choice of the bias input u_0, which provides different steady state values $\bar{W}_0$ for the isolated and connected systems. Note that too large values of u_0 will result in an almost zero response of the loaded system (left side plot of Figure S 1). If u_0 is sufficiently small, $K_2 \ll \bar{W}_0$, and $(W_T - \bar{W}_0) < K_1$, the cycle flux can be well approximated by

$$\delta^C \approx \frac{k'_D}{k'_D + u_0} \frac{\bar{K}_1}{(\bar{K}_1 + (W_T - \bar{W}_0))^2},$$

which is a monotonically decreasing function of the load λ. Hence, we obtain that $\delta^C < \delta^I$ and that $\omega_B^C < \omega_B^I$, that is, the bandwidth of the connected system is smaller than the bandwidth of the isolated system. A more general analysis of the single load system considering large amplitude deviations from the equilibrium is dealt with in the next section.

Figure 3 summarizes the behavior of the bandwidth as a function of the load, the Michaelis-Menten constants, and the input amplitude.

1.4.1 Effects of the enzymes amounts

Case 1 (Double load and ultrasensitive isolated system steady state response: $K_1, K_2 \ll W_T$) We next study the effect of the enzyme amounts, specifically of V_1 and V_2, on the relative difference $\Delta = \frac{A^I(\omega) - A^C(\omega)}{A^I(\omega)}$ between the amplitudes of the isolated and connected systems. Letting for simplicity $V_2 = aV_1$ and $V_1 = V$, we have for sufficiently large frequency ω that $\Delta = 1 - \frac{\beta^C \omega}{\beta^I \sqrt{w^2 + (\delta^C)^2}}$, which decreases as V decreases (because $\frac{\beta^C \omega}{\beta^I \sqrt{w^2 + (\delta^C)^2}}$ increases as V decreases). Hence, as V decreases, that is, the amounts of enzymes decrease, the amplitudes of the connected and isolated system approach each other. This is also shown in Figure S 3. Finally, since the amplitude can never exceed $\min\{\bar{W}_0, W_T - \bar{W}_0\}$, we also have that $A^C(0) \leq A^I(0)$.

Case 2 (Double load and hyperbolic isolated system steady state response: K_1, K_2 comparable with W_T). Furthermore, letting for simplicity $V_2 = aV_1$ and $V_1 = V$, we have for sufficiently large frequency ω that $\Delta = 1 - \frac{\beta^C \sqrt{w^2 + (\delta^I)^2}}{\beta^I \sqrt{w^2 + (\delta^C)^2}}$, which, since $\delta^C < \delta^I$, is an increasing function of V (because $\frac{\beta^C \sqrt{w^2 + (\delta^I)^2}}{\beta^I \sqrt{w^2 + (\delta^C)^2}}$ is a decreasing function of V). As a consequence, when the value of V_1 decreases, that is, the amounts of enzymes decrease, the amplitudes of the connected and isolated systems become further apart from each other. This is opposite to the result obtained for Case 1. Furthermore, when $\omega \to 0$ the behavior of $\bar{W}(t)$ is practically at the quasi steady state and hence it exactly tracks the steady state characteristics of the right-side plot of Figure S 1. Hence, the amplitude of the response of the connected system is smaller than that of the isolated system, that is, $A^C(0) \leq A^I(0)$.

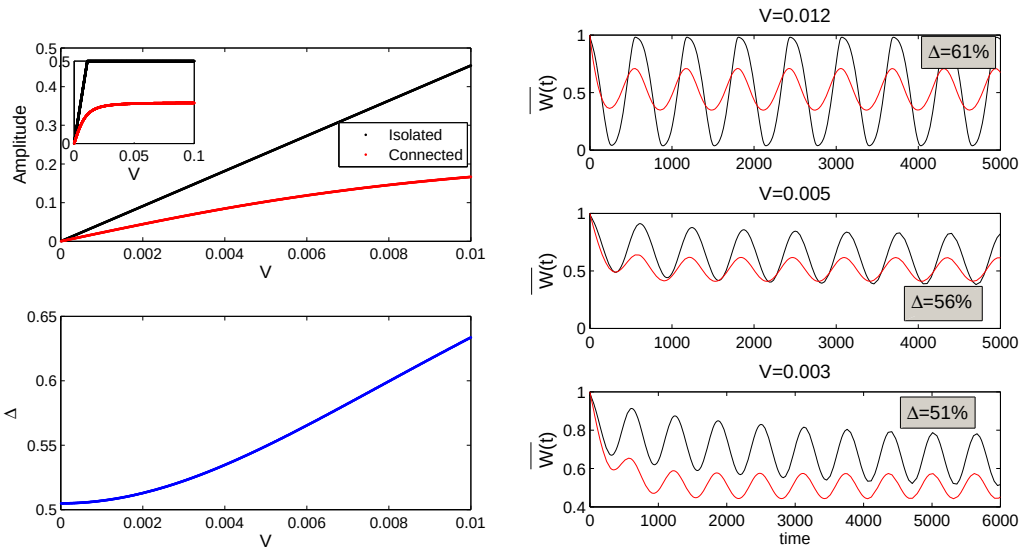

Figure S 3: **Effects of enzymes amounts.** In the left plots, we show the behavior of the amplitudes of the connected (red) and isolated (black) systems as function of V as obtained from the analytical expressions of Table 1. Here, Δ is the difference between the isolated and connected system amplitudes divided by the amplitude of the isolated system. It represents the percentage difference between the amplitudes in the two systems. In the right-side plots, we show data obtained through numerical simulation for three different values of V. As predicted from the analytical expressions, as V decreases, the percentage difference between the two amplitudes decreases. Here, we have set $A_0 = 0.5, u_0 = 1$, $k'_D = \bar{k}'_D = 2$, $K_1 = K_2 = 0.01$, $V_2 = \bar{k}'_D V_1$, $V_1 = V$, $\omega = 0.01$, $\alpha = \lambda = 50$, $W_T = 1$.

Case 3 (Single load). Since $\delta^C < \delta^I$, we have that $\Delta = 1 - \frac{\beta^C \sqrt{w^2+(\delta^I)^2}}{\beta^I \sqrt{w^2+(\delta^C)^2}}$ is an increasing function of V. Hence, as the amounts of enzymes decrease, the amplitudes of the connected and isolated systems become further apart from each other.

The results are summarized in Figure 3 D.

1.5 Input Stimuli as Trains of Pulses with Saturating Amplitudes

In the previous section, we have analyzed the response of the system to periodic (sinusoidal) input profiles of small amplitude of period $T = 2\pi/\omega$. In this section, we consider input stimuli in the form of pulses of large amplitude applied at periods of length T. We assume each pulse to have an exponential profile, that is, $u_M e^{-lt}$, in which u_M is the pulse height and $l > 0$ is the decay rate of the pulse. The input stimulus can be thus written as

$$u(t) = u_0 + u_M \sum_{k=0}^{\infty} e^{-l(t-kT)} 1(t - KT),$$

in which $1(t - kT) = 0$ if $t < kT$ and $1(t - kT) = 1$ otherwise. These types of inputs are more realistic than sinusoidal inputs and in particular are those found in the experiments that we performed. Although the general findings about the effects of targets on the amplitude

and bandwidth of the previous section carry to general types of inputs (as any input can be expressed as an infinite combination of sinusoidal functions), in this and the next section we seek to specifically determine the effect of both u_M and l on the amplitude of response to the pulse.

In this section, we assume that the pulse height u_M and the decay rates are comparably large enough ($u_M \gg k'_D, \bar{k}'_D$ and $l \gg 1$) so that that there are time intervals T_1 and T_2 with $T_1 + T_2 = T$ such that in any period of length T we have that $\frac{V_1}{(1+u/k'_D)} \approx 0$ and $\left(\frac{V_2 u}{k'_D+u}\right) \approx V_2$ for T_1 seconds, while $\frac{V_1}{(1+u/k'_D)} \approx V_1$ and $\left(\frac{u}{k'_D+u}\right) \approx 0$ for T_2 seconds. In such a case, the amplitude of the response can be calculated by directly integrating equation (2) under the assumptions that the steady state characteristics of the isolated system are in the ultrasensitive regime ($K_1, K_2 \ll W_T$) and that for the loaded system, the load is sufficiently large.

Let $t_0, t_0+T, t_0+2T, ..., t_0+kT$ be the sequence of times at which the input pulse is applied. Assuming the pulse height is very large, we approximate the dynamics of the system for every $k > 0$ by

$$\frac{d\bar{W}}{dt} = -V_2 \frac{\bar{W}}{K_2(1+\alpha) + \bar{W}}, \text{ for } t \in [t_0 + kT, t_0 + kT + T_1]$$

$$\frac{d\bar{W}}{dt} = V_1 \frac{W_T - \bar{W}}{K_1(\lambda+1) + (W_T - \bar{W})}, \text{ for } t \in [t_0 + kT + T_1, t_0 + kT + T_1 + T_2],$$

in which T_1 is the duration of time in which the approximation $\frac{V_2 u}{(\bar{k}'_D+u)} \approx V_2$ and $\frac{V_1}{(1+u/k'_D)} \approx 0$ hold and $T_1 + T_2 = T$. Under this approximation, we can integrate the above differential equations to obtain (letting $\bar{K}_1 = K_1(1+\lambda)$ and $\bar{K}_2 = K_2(1+\alpha)$) the following algebraic equations for the lower peaks $\bar{W}(t_0 + kT + T_1)$ and for the upper peaks $\bar{W}(t_0 + kT)$, with $\bar{W}(t_0) = W_T$

$$\bar{K}_2 \ln\left(\frac{\bar{W}(t_0 + kT + T_1)}{\bar{W}(t_0 + kT)}\right) + \bar{W}(t_0 + kT + T_1) - \bar{W}(t_0 + kT) + V_2 T_1 = 0, \tag{15}$$

and

$$\bar{K}_1 \ln\left(\frac{W_T - \bar{W}(t_0 + kT + T_1)}{W_T - \bar{W}(t_0 + (k+1)T)}\right) + \bar{W}(t_0 + (k+1)T) - \bar{W}(t_0 + kT + T_1) - V_1 T_2 = 0, \tag{16}$$

respectively. Now, we study the isolated and connected system cases separately.

Isolated System. Since the isolated system is assumed to operate in the ultrasensitive regime, we have that $K_1, K_2 \ll W_T$. We can thus neglect in expressions (15-16) the terms multiplying K_1 and K_2 so that we obtain the sequences of the upper peaks as

$$\{W_T, W_T - V_2T_1 + V_1T_2, W_T - 2V_2T_1 + 2V_1T_2, ..., W_T - kV_2T_1 + kV_1T_2\}$$

and for the lower peaks as

$$\{W_T - V_2T_1, W_T - 2V_2T_1 + V_1T_2, W_T - 3V_2T_1 + 2V_1T_2, ..., W_T - (k+1)V_2T_1 + kV_1T_2\}.$$

So, by taking the difference between the upper peaks and lower peaks and considering that this difference cannot exceed W_T, we obtain the following expression for the difference between the

upper and lower peaks:

$$A = \begin{cases} V_1T_2 & \text{if } V_2T_1 \geq V_1T_2 \text{ and } W_T \geq V_1T_2 \\ W_T & \text{if } V_2T_1 > V_1T_2 \text{ and } W_T < V_1T_2 \\ \min\{W_T, V_2T_1\} & \text{if } V_2T_1 < V_1T_2 \text{ and } V_2T_1 > W_T \\ \min\{W_T, V_2T_1\} & \text{if } V_2T_1 < V_1T_2 \text{ and } V_2T_1 < W_T, \end{cases}$$

from which, merging the second to last case, we obtain that

$$A = \begin{cases} V_1T_2 & \text{if } V_2T_1 \geq V_1T_2 \text{ and } W_T \geq V_1T_2 \\ \min\{W_T, V_2T_1\} & \text{if } V_2T_1 < V_1T_2 \text{ or } V_2T_1 > V_1T_2 > W_T, \end{cases}$$

which, simplifying the conditions of the cases, finally leads to

$$A = \begin{cases} V_1T_2 & \text{if } V_1T_2 \leq \min\{W_T, V_2T_1\} \\ \min\{W_T, V_2T_1\} & \text{if } V_1T_2 > \min\{W_T, V_2T_1\}, \end{cases}$$

from which, substituting $T_2 = 2\pi/\omega - T_1$, we obtain the final expression for the amplitude as

$$A^I(\omega) = \begin{cases} \min\{V_2T_1, W_T\} & \text{if } \omega \leq \frac{2\pi V_1}{T_1V_1 + \min\{T_1V_2, W_T\}} \\ \frac{2\pi V_1}{\omega} - V_1T_1 & \text{if } \omega > \frac{2\pi V_1}{T_1V_1 + \min\{T_1V_2, W_T\}}, \end{cases} \tag{17}$$

in which the bandwidth ω_B^I is given by

$$\omega_B^I = \frac{2\sqrt{2}\pi V_1}{T_1V_1 + \sqrt{2}\min\{T_1V_2, W_T\}}.$$

Expression (17) is a good approximation, especially at low frequencies as seen in Figure S 4 and hence it is a suitable means for calculating the bandwidth of the isolated system. The analytical expression of the amplitude reaches zero for the value of ω such that $T_2 = 0$ because in such a case the effective input to the system also has zero amplitude.

Connected System (double load). For the connected system, assuming the load is sufficiently large, the values of $\bar{K}_1$ and $\bar{K}_2$ are large enough so that in expressions (15-16) we can neglect the linear terms. This way, denoting by $\lambda_1 = V_2T_1/\bar{K}_2$ and by $\lambda_2 = V_1T_2/\bar{K}_1$, we obtain the sequence of upper peak values as

$$\{W_T, W_T(1 - e^{-\lambda_2} + e^{-(\lambda_1+\lambda_2)}), W_T(1 - e^{-\lambda_2} + e^{-(\lambda_1+\lambda_2)} - e^{-(\lambda_1+2\lambda_2)} + e^{-(2\lambda_1+2\lambda_2)}), ...\}.$$

In particular, one can calculate the limit of this sequence by using the limit of a geometric series and obtain that the upper peaks tend to

$$W_T\left(1 - \frac{(1 - e^{-\lambda_1})e^{-\lambda_2}}{1 - e^{-\lambda_2-\lambda_1}}\right).$$

Similarly, the sequence of lower peaks is given by

$$\{W_Te^{-\lambda_1}, W_T(e^{-\lambda_1} - e^{-(\lambda_1+\lambda_2)} + e^{-(2\lambda_1+\lambda_2)}), ...\},$$

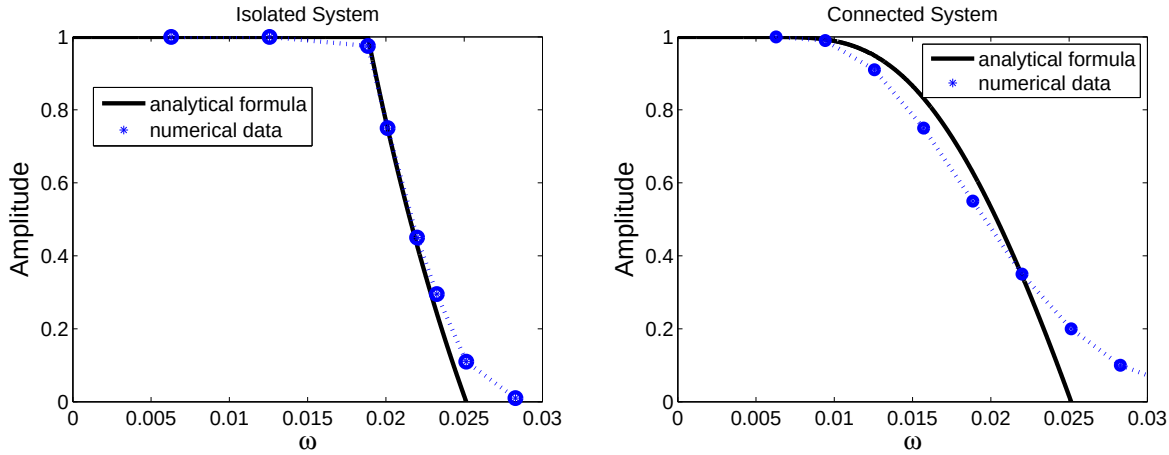

Figure S 4: **Effect of the load on the amplitude of response to a train of pulses.** the left plots, we show the behavior of the amplitude of the isolated system of equation (17) (solid) compared to numerical simulation data (dashed) obtained for $u(t)$ equal to a train of pulses of width equal to $T_1 = 250$. In the right-side plots we show the behavior of the amplitude of the connected system of equation (18) (solid) compared to numerical simulation data (dashed). Here, we have set $k'_D = \bar{k}'_D = 2$, $K_1 = K_2 = 0.01$, $V2 = \bar{k}'_D V_1$, $V_1 = V = 0.012$, $\alpha = \lambda = 100$, $W_T = 1$.

which is also a monotonically decreasing sequence. Its limit can be computed by using again the limit of a geometric series to obtain

$$W_T \left(1 - \frac{1 - e^{-\lambda_1}}{1 - e^{-\lambda_2 - \lambda_1}}\right).$$

By computing the difference between the limit of the lower peaks and the limit of the upper peaks and letting $\lambda_1 = V_2 T_1 / \bar{K}_2$ and $\lambda_2 = V_1 T_2 / \bar{K}_1$, we obtain

$$A^C(\omega) = W_T \frac{(1 - e^{-\lambda_1})(1 - e^{-V_1/\bar{K}_1(2\pi/\omega - T_1)})}{1 - e^{-\lambda_1 - V_1/\bar{K}_1(2\pi/\omega - T_1)}}, \tag{18}$$

which is a good approximation for sufficiently large values of T_2, that is, for sufficiently low frequencies (right-side plot of Figure S 4). Hence, it is a suitable expression for calculating the bandwidth of the system. For values of T_2 approaching zero, the analytical expression of the amplitude approaches zero because $\frac{V_1}{(1+u/k'_D)} \approx 0$ and $\left(\frac{u}{k'_D + u}\right) \approx V_2$ for all t and thus also the stimulation has effectively zero amplitude. The expression (18) can be employed to calculate the bandwidth of the system as

$$\omega_B^C = \frac{2\pi V_1}{V_1 T_1 + \bar{K}_1 \ln\left(\frac{\sqrt{2} - e^{-\lambda_1}}{\sqrt{2} - 1}\right)},$$

which becomes smaller as T_1 and/or the load increases. In particular, as λ increases, this bandwidth monotonically decreases, but as α increases also, the decrease of this bandwidth is not as dramatic. Hence, when the load applied to W is much larger than the load applied to W*, the decrease of bandwidth due to the load is more dramatic. In particular, the above

expression holds when the load on both W and W* is large enough. In this case, we have that $\bar{K}_1 \ln\left(\frac{\sqrt{2}-e^{-\lambda_1}}{\sqrt{2}-1}\right) \approx \frac{K_1(1+\lambda)}{K_2(1+\alpha)}\frac{V_2T_1}{\sqrt{2}-1}$. Hence, the value of ω_B^C is smaller than that of ω_B^I as long as $\frac{K_1(1+\lambda)}{K_2(1+\alpha)} > \sqrt{2}-1$.

By contrast, if the load is applied to W only, that is, $\alpha = 0$, we obtain the following approximated expressions for the amplitude and bandwidth, respectively (see the Appendix for the derivations):

$$A^C(\omega) = \begin{cases} V_2T_1 & \text{if } \omega \leq \omega_B^C \\ W_T(1-\exp\left(-\frac{V_1}{K_1}(\frac{2\pi}{\omega}-T_1)\right) & \text{if } \omega > \omega_B^C, \end{cases} \tag{19}$$

in which

$$\omega_C^B = \frac{2\pi V_1}{V_1T_1 + \bar{K}_1 \ln\left(\frac{1}{1-V_2T_1/W_T}\right)}. \tag{20}$$

Connected system (single load: $\alpha = 0$). In this case, we have that $\bar{K}_1 = K_1$ and assuming still that the system operates in the ultrasensitive regime ($K_1, K_2 \ll W_T$), we obtain the amplitude as

$$A^C(\omega) = \begin{cases} V_2T_1 & \text{if } \omega \leq \frac{2\pi V_1}{V_1T_1+\bar{K}_1\ln\left(\frac{1}{1-V_2T_1/W_T}\right)} \\ W_T(1-\exp(-\frac{V_1(2\pi/\omega-T_1)}{\bar{K}_1})) & \text{if } \omega > \frac{2\pi V_1}{V_1T_1+\bar{K}_1\ln\left(\frac{1}{1-V_2T_1/W_T}\right)}, \end{cases} \tag{21}$$

from which the bandwidth is computed as

$$\omega_B^C = \frac{2\pi V_1}{V_1T_1 + \bar{K}_1 \ln\left(\frac{1}{1-V_2T_1/(\sqrt{2}W_T)}\right)}. \tag{22}$$

This bandwidth monotonically decreases with the load λ.

Summary. When the load is applied to both W and W*, if K_1 and K_2 are the same, and the load is equally distributed between W and W*, then the bandwidth of the connected system is lower than that of the isolated system. In general, when the effective Michaelis-Menten constant of the forward reaction in the loaded system, that is, $K_1(1+\lambda)$, is larger than the effective Michaelis-Menten constant of the backward reaction, that is, $K_2(1+\alpha)$, then the loaded system will display a smaller bandwidth. In Figure S 4, for example, the bandwidth of the loaded system is much smaller than that of the isolated system. When the load is applied to W only, the bandwidth is a monotonically decreasing function of the load λ. Comparing expression (22) to expression (20), it follows that if $\alpha \approx \lambda$, the bandwidth decreases more dramatically in the system with single load than in the system with double load when the load λ increases.

We finally examine the trend of the upper and lower peaks of the responses as well as the bias level of the response when both α and λ are nonzero.

Peaks. The values of the upper and lower peaks for both the isolated and connected systems monotonically decrease and approach each other for high enough values of the frequency of the input stimulation. Therefore, for high enough values of the frequency, the response of both the connected and isolated systems will tend to constant values, which are the smallest values each of the systems (isolated and connected) can reach.

Bias level. The value of the enzyme amounts, that is, the value of V influences the relative location of the bias values of the signals subject to periodic input stimuli. Specifically, the location of the lower peaks of the isolated system when $V_1T_2 > V_2T_1$ is given by $W_T - V_2T_1$. By contrast, the lower peaks of the connected system are at $W_T(1 - \frac{1-e^{-\lambda_1}}{1-e^{-\lambda_1-\lambda_2}})$, in which $\lambda_1 = V_2T_1/\bar{K}_2$ and $\lambda_2 = V_1T_2/\bar{K}_1$. If $V_2 = aV_1$ and $V_1 = V$ with V very small, this expression is well approximated by $W_T\left(\frac{T_2/\bar{K}_1}{aT_1/\bar{K}_2+T_2/\bar{K}_1}\right)$. For V small enough, we thus have that $W_T - aVT_1 > W_T\left(\frac{T_2/\bar{K}_1}{aT_1/\bar{K}_2+T_2/\bar{K}_1}\right)$, which implies that the bias of the connected system response will be smaller than the bias of the isolated system response.

The bias level is also affected by the frequency ω. Specifically, when ω increases we have that T_2 becomes very small and approaches zero. When T_2 approaches zero, we have that $-V_2\left(\frac{u}{k'_D+u}\right) \approx -V_2$ while $\frac{V_1}{(1+u/k'_D)} \approx 0$ for all time. If there is a basal level V_0 for the forward reaction, the dynamics of both the connected and isolated systems are given by

$$\frac{d\bar{W}}{dt} = -V_2\frac{\bar{W}}{\bar{K}_2 + \bar{W}} + V_0.$$

Starting from $\bar{W}(0) = W_T$, the system reaches the steady state $\bar{W} = \frac{V_0}{V_1-V_0}\bar{K}_2$. Since $\bar{K}_2 = K_2(1+\alpha)$ and $\alpha = 0$ for the system without the load, then the final steady state reached for the isolated system is higher than the final steady state reached by the connected system.

2 Experimental Systems

In this section, we describe in more detail the development of the experimental system for measurement of responses to time-varying input stimulation by the reconstituted UTase/UR-PII cycle and provide additional data on the response time.

In addition to the two experiments that were averaged in Figure 4 E, we examined the decay time in experiments where glutamine was added to 0.5 mM, 0.8 mM, and 1.5 mM, all of which are non-saturating levels of stimulation. Hence, the cycle operates in the first-order regime. Conditions for these experiments are in the legend for Figure S 5. As shown in Figure S 5, when glutamine was added to 0.5 mM, we could not detect a difference in decay time between isolated and connected systems. When glutamine was injected to 0.8 mM, the isolated system appeared to be slower than did the isolated system. When glutamine was injected to 1.5 mM, the connected system again appeared to be faster than the isolated system, but only marginally so (Figure S 5). Thus, targets could speed up the response to stimulation with intermediate glutamine concentrations, but only within a narrow range of the intermediate glutamine concentrations.

The rise time of the system was also observed under conditions of intermediate stimulation, using both wild-type and heterotrimeric PII and at a variety of glutamine concentrations. These experiments were conducted using the same conditions described for measuring rise-time in the main text, except that intermediate concentrations of glutamine were present. As shown in Table 2, under no conditions did we identify a glutamine concentration at which the rise time of the connected system was faster than was the rise time of the isolated system. The general trend was that the difference between isolated and connected system became smaller as the glutamine concentration was increased (Table 1). Thus, in our experimental system targets

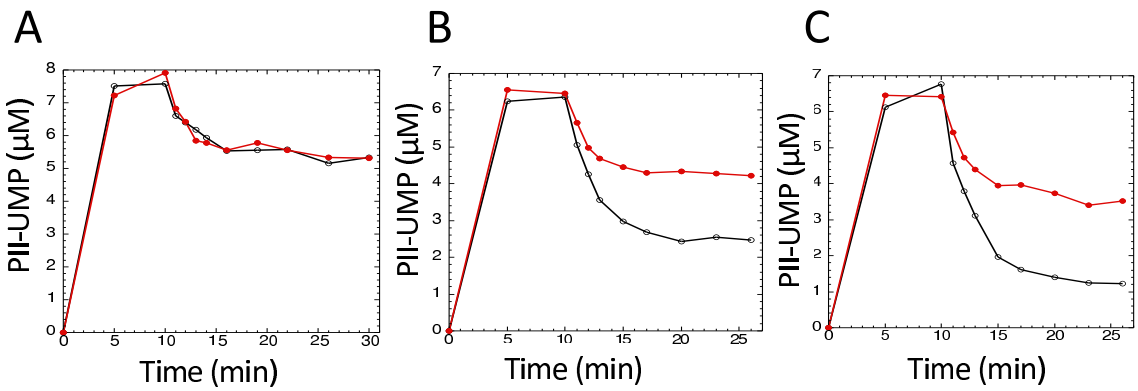

Figure S 5: **Response of the UTase/UR-PII cycle to stimulation with nonsaturating concentrations of glutamine.** Reaction conditions were 100 mM Tris-Cl, pH 7.5, 100 mM KCl, 10 mM MgCl, 0.3 mg/mL bovine serum albumin, 3 μM PII, 1.5 μM UTase/UR, 0.2 mM α-ketoglutarate, 1 mM UTP, 1 mM ATP, and NRII at 0 (black curves and points) or 10 μM (red curves and points). Reactions were incubated in the absence of glutamine for 10 min, after which glutamine was added. A. Glutamine was added to 0.5 mM. B. Glutamine was added to 0.8 mM. C. Glutamine was added to 1.5 mM. Note that panel B is a different experiment than the two experiments used to produce Figure 4 E in the main text, and thus serves as an additional repeat of that experiment.

had an asymmetrical effect upon intermediate stimulation (at 0.8 mM glutamine), it made responses faster in one direction while making responses in the opposite direction slower.

To impose a relaxation oscillator-type time-varying input signal, we included an enzyme that consumes glutamine in the reaction mixtures, and periodically injected glutamine into the system. Suitable glutaminase enzymes were not available commercially, as we required an enzyme with a low K_m to efficiently remove low concentrations of glutamine from our systems, and the enzyme must have sufficient catalytic rate to efficiently operate in the time frame of our *in vitro* experiments. A useful glutaminase proved to be the pyridoxal phosphate synthase from the thermophile *Geobacillus stearothermophilus*; we used this enzyme in the absence of its other targets, ribose-5-phosphate and glyceraldehyde-3-phosphate because additional studies showed that these, curiously, decreased the rate of glutamine consumption. The pyridoxal phosphate synthase (PLPS) consists of two types of subunits (S and T) forming a 24-mer, in which the T subunits catalyze glutamine conversion to glutamate, but only when in the 24-mer. In some experiments, we added additional T subunits to ensure that the 24-mer was saturated with this subunit. Figure S 6 shows how this glutaminase can be used to create time-varying input signals. In the two experiments shown, uridylylation of PII was allowed to occur in the absence of glutamine, resulting in complete modification of PII, and glutamine was injected when shown by the arrow. In Figure S 6A, the reaction mixtures contained different levels of glutaminase, and a low concentration of glutamine was injected (2.5 mM). When no glutaminase was present, PII uridylylation state fell to the low level characteristic of 2.5 mM glutamine, and stayed there (bottom curve). As glutaminase was increased, increasingly shallow dips in the level of PII uridylylation were observed. That is, as the rate of decay of the input signal (glutamine) was increased, the amplitude of response decreased as expected from our theoretical analysis. In Figure S 6B, a saturating glutamine concentration was injected (5

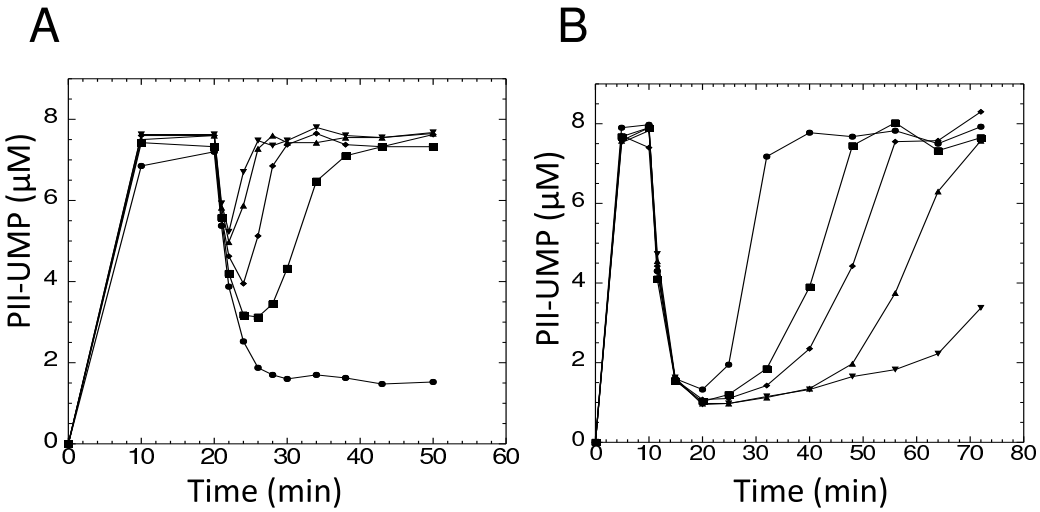

Figure S 6: **Using glutaminase and injections of glutamine to impose time-varying input stimulation**. A. Amplitude and time-course of the response to glutamine injection depend upon the concentration of glutaminase and attendant rate of glutamine decay. The UTase/UR-PII monocycle was incubated in the absence of glutamine for 20 min and with different amounts of glutaminase present, allowing PII to become fully modified, after which glutamine was added to 2.5 mM (indicated by arrow). After the addition of glutamine, the amplitude of the response and the time it took for PII to become uridylylated again depended upon the amount of glutaminase that was present. Reaction conditions were: 100 mM Tris-Cl, pH 7.5, 100 mM KCl, 10 mM MgCl, 0.3 mg/mL bovine serum albumin, 3 μM PII, 1.5 μM UTase/UR, 0.2 mM α-ketoglutarate, 1 mM UTP, 1 mM ATP, and pyridoxyl phosphate synthase (all PLPS amounts stated include additional PdxT subunits in ratio PLPS 1: "extra" PdxT 0.2 to ensure saturation of enzyme with the PdxT subunit). The PLPS concentrations were (from lowest to highest curve) 0 μM, 50 μM, 100 μM, 150 μM, and 200 μM. B. At saturating stimulation, the time-course of the response depends upon the concentration of glutaminase present. Reaction mixtures were as above except lacking glutaminase, and were incubated in the absence of glutamine, allowing PII to become fully modified. After 10 min, glutamine was added to 5 mM, and simultaneously different concentrations of glutaminase were added. The glutaminase in this case consisted of purified PLPS 24-mer without addition of extra PdxT subunits. The time required for restoration of PII-UMP depended upon the concentration of glutaminase added; these concentrations were (fastest curves to slowest) 100 μM, 60 μM, 50 μM, 40 μM, and 30 μM.

mM), along with different levels of the glutaminase protein. In this case, the time required for the system to recover from the glutamine addition depended upon the level of glutaminase. In both experiments, the level of PII uridylylation eventually returned to the level obtained in the absence of glutamine, signifying that the K_m of the glutaminase is sufficiently low as to allow removal of glutamine from the reaction mixtures.

Measurement of the amplitudes of responses after glutamine addition proved to be dependent upon whether or not the system had attained a steady state prior to the first addition of glutamine. This issue is illustrated in Figure S 7. When the system had attained a steady state prior to the first addition of glutamine, the amplitude of the initial response was similar to

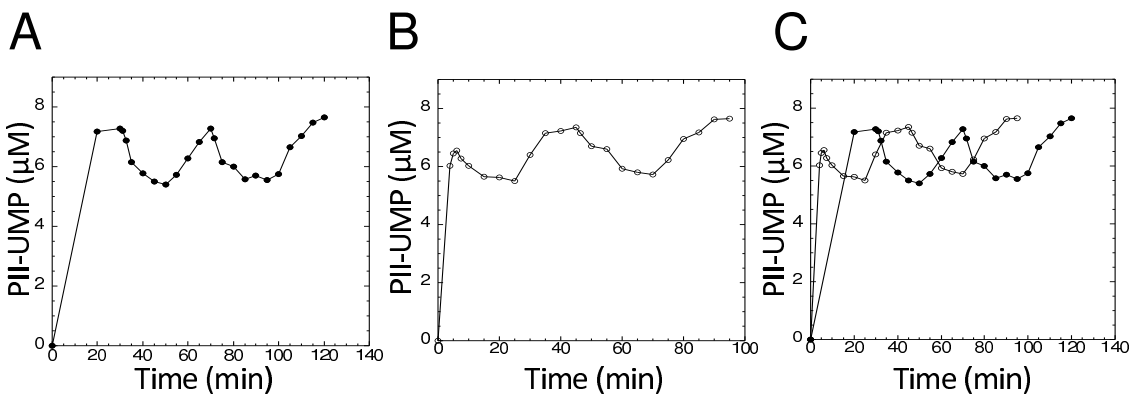

Figure S 7: **Amplitude of the initial response to glutamine addition depends on whether or not the system has achieved a steady state before glutamine addition.** Identical reaction conditions were used for the experiments shown in panels A and B, and panel C shows an overlay of these results. Reaction conditions were: 100 mM Tris-Cl, pH 7.5, 100 mM KCl, 10 mM MgCl, 0.3 mg/mL bovine serum albumin, 3 μM PII, 0.1 μM UTase/UR, 0.2 mM α-ketoglutarate, 1 mM UTP, 1 mM ATP, 10 μM NRII, 75 μM PLPS, and additional 15 μM pdxT subunit of PLPS. For panel A, the reaction mixture was incubated for 30 min in the absence of glutamine, after which glutamine was added to 5 mM at 30 min and again at 70 min. In this experiment, the system had achieved the steady state prior to the first addition of glutamine. For panel B, the reaction mixture was incubated for 5 min in the absence of glutamine, after which glutamine was added to 5 mM. A second injection of glutamine to 5 mM occurred at 45 min. In this experiment, the system had not yet attained the steady state at the 5 min point when the first addition of glutamine occurred. As shown in panel C, the amplitudes of the second response were similar, but the amplitudes of the first response were not, suggesting that amplitudes for the first response are strongly affected by whether the system had achieved the steady state.

that of a later injection of glutamine. However, a smaller amplitude of the initial response to glutamine was observed if the system had not yet attained the steady state prior to challenge with glutamine, while a later challenge in the same experiment yielded a response with higher amplitude (Figure S 7). Thus, the amplitude of the first response is unreliable, unless it is certain that the steady state had been attained before addition of glutamine. Because of this, we routinely ignored the first decay upon addition of glutamine, and measured amplitudes starting with the first rise in PII-UMP after glutamine addition.

References

[1] L. B. Bushard. Comparison theorems for scalar and vector second order nonlinear ordinary differential equations and inequalities. *Journal of Mathematical Analysis and Applications*, 52:561–572, 1975.

[2] A. Goldbeter and D. E. Koshland. An amplified sensitivity arising from covalent modification in biological systems. *Proc. Natl. Acad. Sci. USA*, pages 6840–6844, 1981.

[3] C. Gomez-Uribe, G. C. Verghese, and L. A. Mirny. Operating regimes of signaling cycles: Statics, dynamics, and noise filtering. *PLOS Computational Biology*, 3(12):2487–2497, 2007.

[4] H. Khalil. *Nonlinear Systems*. Prentice Hall, 2002.

[5] E. Klipp, R. Herwig, A. Kowald, C. Wierling, and H. Lehrach. *Systems Biology in Practice*. Wiley, 2005.

[6] G. Russo, M. di Bernardo, and E. D. Sontag. Global entrainment of transcriptional systems to periodic inputs. *Plos Computational Biology*, 2010.

[7] A. C. Ventura, P. Jiang, L. Van Wassenhove, D. Del Vecchio, S. D. Merajver, and A. J. Ninfa. Signaling properties of a covalent modification cycle are altered by a downstream target. *Proc. Natl. Acad. Sci. USA*, 107(22):10032–10037, 2010.